Modeling and analysis of E-shaped birefringent photonic crystal fiber for temperature sensing applications

MANISHA SINGH[1,*], SHIPRA[2], SHAHIRUDDIN[3]
[1]*Department of Electronics and Communication Engineering, Birla Institute of Technology, Patna Campus, Patna 800014, India*
[2]*Department of Electronics and Communication Engineering, Birla Institute of Technology, Patna Campus, Patna 800014, India*
[3]*Department of Electronics and Communication Engineering, Bakhtiyarpur College of Engineering, Bakhtiyarpur 803212, India*

In many medicinal, environmental, and industrial applications, temperature measurement is a crucial parameter that needs to be monitored. A temperature-sensing E-shaped photonic crystal fiber is designed, with the core initially filled with air and compared the outcome with the core filled with propanol. With an emphasis on their structure, sensing processes and performance characteristics, this research investigates the integration of PCF for sensing temperature. The proposed E-shaped PCF is simulated using finite element method (FEM) in R-soft software. For both air-filled core and propanol filled core, different parameters such as birefringence, temperature, and temperature sensitivity are calculated at different wavelength ranging from 1 μm to 1.7 μm. The sensitivity of the designed structure ranges from -1.439 nm/˚C to -1.192 nm/˚C after filling propanol in the wavelength 1 μm to 1.7 μm range. And for air filled PCF the sensitivity of the designed structure ranges from -1.491 nm/˚C to -1.281 nm/˚C in the same wavelength from 1 μm to 1.7 μm range. The higher value of Birefringence is 7.62×10^{-2} which is calculated after filling propanol and that of for air filled air hole is 6.61×10^{-2}. The main aim of the designed PCF is to focus on their potential as next-generation sensors that can overcome the drawbacks of conventional temperature sensor while providing greater functionality and versatility.

(Received August 12, 2025; accepted February 2, 2026)

Keywords: Photonic crystal fiber, Finite element method, Temperature sensitivity

1. Introduction

Photonic crystal fibers (PCFs), a class of optical fibers distinguished by their unique micro structured designs, have garnered significant attention in recent years for various sensing applications, including temperature measurement. Temperature sensing is crucial in many fields, including biomedical applications, environmental science, and industrial monitoring. Conventional temperature sensors frequently have issues with sensitivity, spatial resolution, and range. However, compared to traditional sensing techniques, photonic crystal fibers provide a number of benefits, including increased sensitivity, the possibility of downsizing, and the capacity to function in challenging or remote situations. Because of their unique optical characteristics, temperature sensors can precisely detect even the smallest temperature changes which have been developed. Specifically, the PCF's usage in temperature sensing is based on the interaction between light and its structure, such as the shifting of resonant wavelengths brought on by temperature-related changes in the refractive index of the fibre. The ability to tailor the fiber's geometry and material properties makes PCFs ideal candidates for creating temperature sensors that are both highly sensitive and versatile. PCFs provide excellent guiding mechanism and flexibility in a number of design factors, such as the size and shape of the core and cladding holes for their respective positions. Different shapes as well as arrangements of air holes, affect both the guiding properties and the optical characteristics of the fibre. Certain studies have demonstrated nonlinearity and decreased confinement loss in proportion to increasing birefringence values [1]. Therefore, their confided structure can be freely used for the sensing applications. Although the sensors based on photonics are still in the growing stage [2], the prospects to develop subtypes of sensors, like temperature sensors [3], pressure sensors [4], mechanical sensors [5], gas sensors, and biosensors [6], are very broad. The wearable sensors and biosensors which can be connected either via Bluetooth or directly accessible via a smartphone plays a vital role in today's scenario. Biosensors are bioanalytical tools that are quantitatively designed for the sensitive detection of analytes, and many techniques has been applied to make the biosensor dependable and more efficient over time, as biosensors has to overcome many challenges before, they can be widely used in our day to day lives. Since the thermo-optic and thermal expansion coefficients of silica and air holes in PCF are low, therefore the optical fiber interferometers utilizing PCF have extremely low temperature sensitivity [6-9]. Hence, to improve the PCF's ability to sense changes in external temperature, temperature-sensitive compounds such glycerin, liquid

crystal, and alcohol are frequently injected into the air holes of the PCF.

For the last few years, the PCF for sensing temperature have attracted great intrigue due to their excellent properties such as, light weight, tiny size, capability of remote sensing and immunity to electromagnetic radiation. There are currently many techniques for measuring temperature, such as surface plasmon resonance (SPR) [10], fiber Bragg grating (FBG) [7], long period fiber grating (LPFG) [8], and Sagnac interferometer (SI) [9]. Temperature sensors based on SPR are much more desirable due to ease of use, and high sensitivity, along with label-free measurement abilities. In the SPR phenomenon, the (RI) refractive index used for the sensing medium has a remarkable influence upon it. As a consequence, there is a significant shift in the SPR spectrum because of the change in RI caused by some physical factor. The effect of temperature is among one of these components, and the change of the refractive index (RI) used for the sensing medium varies directly to the value of the thermo-optical coefficient of the medium. Recently, a variety of SPR-based PCF temperature sensors have been introduced [10], in which a temperature-sensitive liquid is poured into all of the PCF's air pores after the metal layer has been overlaid. The tiny diameter of the PCF holes makes it challenging to deposit a metal coating around them and fill them with a liquid that is sensitive to temperature changes. One workable way to address this issue is to build a D-shaped sensor PCF [11]. In the disciplines of biomedicine, these types of PCF are frequently used to track dialysis and medical incubator equipment [12]. In this paper, a E-shaped PCF for temperature sensor based on SPR is designed. The simulations are performed using finite element method (FEM). The main objective of the proposed design is to achieve improved sensitivity in a wide range of temperature. As a result, a slight change in temperature causes the propagation loss peak to move significantly, thus boosting the sensor's sensitivity. Furthermore, the E-shaped PCF0s has many structural features that can be optimized to produce a very high sensitivity that is on par with other developed sensors. It has a wide range of application in the civil, aerospace, and defense industries to monitor and regulate the health of their structures. With so many uses in so many different fields, this type of temperature sensor is among the most in demand in the commercial market also. The suggested sensor can be a suitable option for temperature measurement even in remote sensing applications because of its superior performance and larger temperature range.

2. Proposed design and simulation results

The proposed designed Photonic Crystal Fiber is a E-shaped PCF found for the temperature sensor is shown in the Fig. 1 with its cross -sectional view. The 3-D view of the proposed structure is given in Fig. 2. All the air holes are patterned in a square lattice which finally form an E-shape PCF. The diameter (d) of each air hole is equal to 1 µm, while the pitch (Λ) or the center-to-center distance of the nearby air holes is equal to 1.2 µm. Initially the inner ring from where the light is confined is filled with the propanol having refractive index of 1.38 and besides this all the cladding air holes are filled with air having refractive index 1. Here, the entire cladding region is compressed by the air holes which are red in colour is filled with air and only air holes of the core region are blue in colour is filled with propanol. And all the results were simulated. After that in next step the inner ring is filled with air and all the results are computed without altering the dimensions. These simulated results were compared with the design in which propanol is filled in the core of PCF. Fig. 3(a) and 3(b) indicate the light intensity distribution along x-axis and y-axis of the proposed E-shaped PCF. In this design light is confined mostly in the core of the designed structure. Here, silicon dioxide is used for the background material because of its novel optical behavior, and its dispersion ratio as a function of temperature is calculated by the Sellmeier equation shown in Eq. 1 [13-15]:

$$n^2(\lambda) = 1 + \frac{B_1\lambda^2}{\lambda^2 - C_1} + \frac{B_2\lambda^2}{\lambda^2 - C_2} + \frac{B_3\lambda^2}{\lambda^2 - C_3} \qquad (1)$$

Here n, denotes refractive index (RI) of the silica material and B_1, B_2, B_3, C_1, C_2, and C_3 are the sellmeier coefficients whose values are given as B_1 = 0.696163, B_2 = 0.4079426, B_3 = 0.8974794, C_1= 0.0046914826 µm^2, C_2= 0.0135120631 µm^2, C_3= 97.93400251 µm^2 at a conventional temperature T = 25 °C.

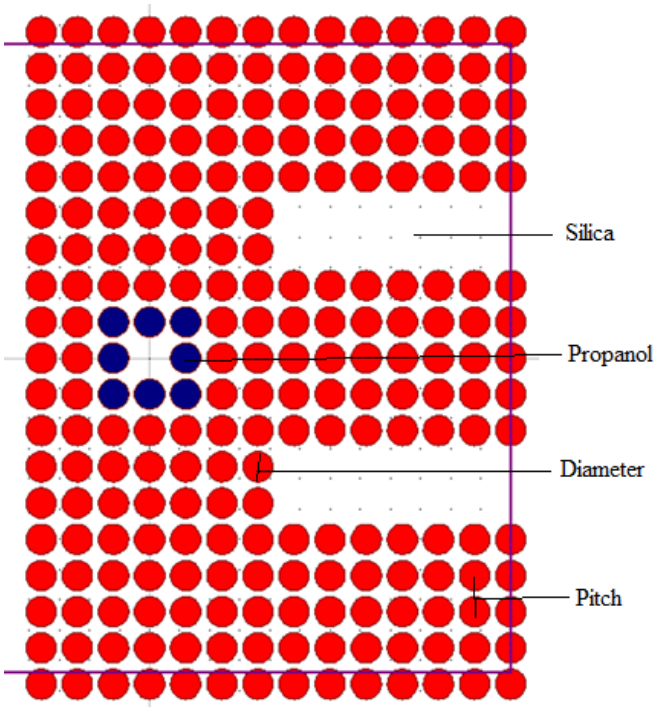

Fig. 1. Cross section of E-shaped structure with d = 1 µm, Λ =1.2 µm for air and propanol filled core (colour online)

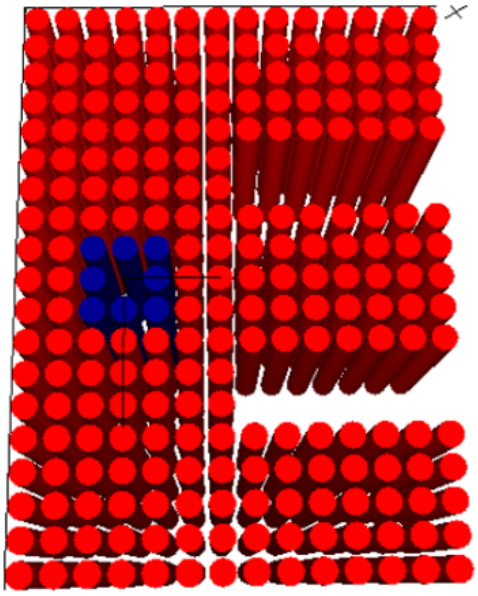

Fig. 2. Three-Dimensional (3-D) view of the proposed design (colour online)

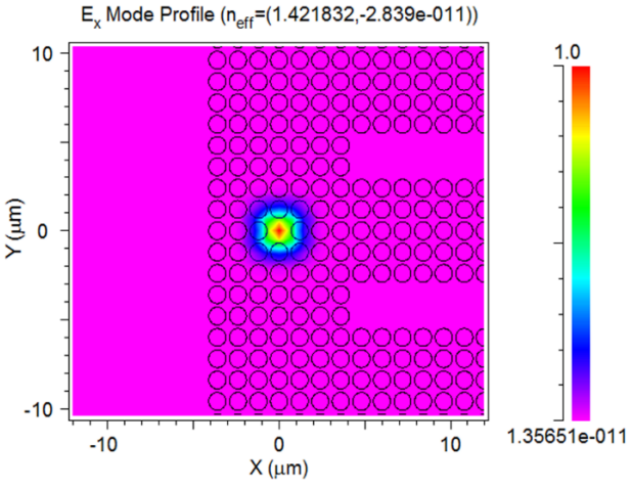

Fig. 3(a). Field intensity distribution of E_x mode (colour online)

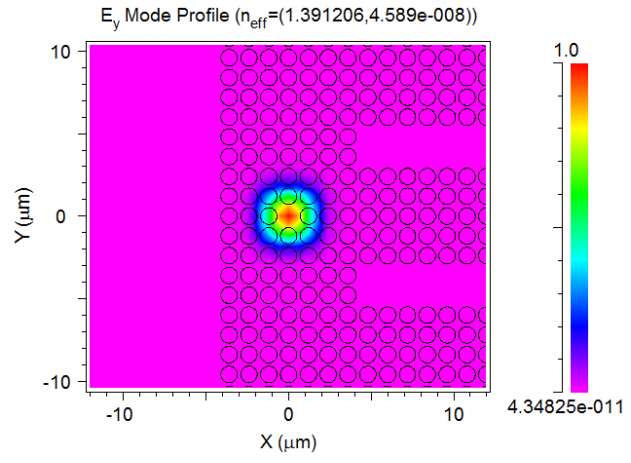

Fig. 3(b). Field intensity distribution of E_y mode (colour online)

3. Theoretical evaluation

Birefringence is an important characteristic of the PCF which depends on effective refractive index differences between the x-polarization and the y polarization and also depends upon the operating wavelength. The formula used for calculating birefringence [12-16] is given below.

$$B = \text{Real}|neff_x - neff_y| \quad (2)$$

where $neff_x$ and $neff_y$ signifies the effective indices in X and Y polarized mode. Fig. 4 shows the graph of Birefringence vs wavelength for air and propanol and it can be visualized from the graph that as the wavelength rises from 1 μm to 1.8 μm the value of Birefringence also risess for air and propanol filled PCF. The suggested structure has a birefringence of about 10^{-2}. Furthermore, the birefringence values rise as the operation wavelength is increased because the light field enters the asymmetrical cladding region more deeply. However, the birefringence of the suggested PCF reduces especially at long wavelengths after air is introduced into the airholes. At wavelength 1.8 μm the higher value of Birefringence is 7.62×10^{-2} which is calculated after filling propanol and that of for air is 6.61×10^{-2}. Here we have utilized the (FEM) finite element method to analyze the modal birefringence of proposed PCF based temperature sensor. These computations have been accomplished using Rsoft software.

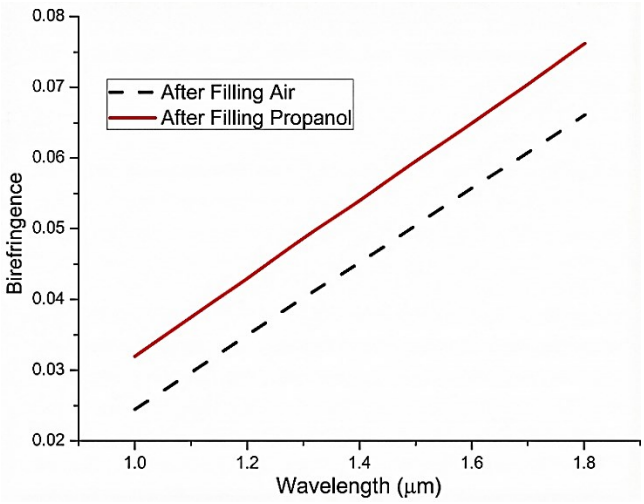

Fig. 4. Birefringence vs. Wavelength (colour online)

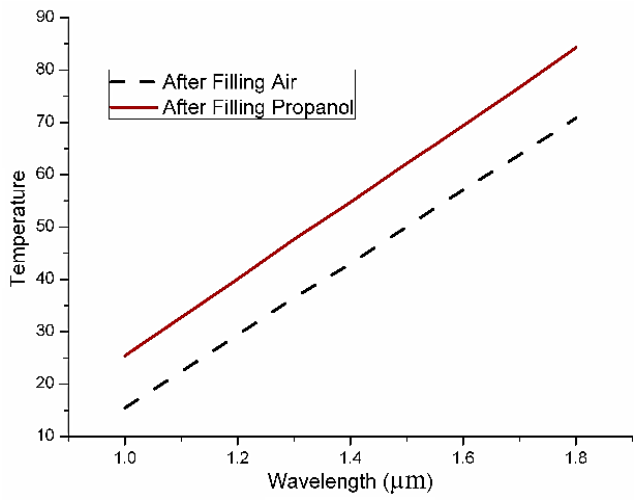

Fig. 5. Temperature (^{o}C) vs. Wavelength (μm) (colour online)

The graph depicted above in Fig. 5 is the temperature versus wavelength graph of the proposed E-shaped PCF. Here temperature varies accordingly with the wavelength as the wavelength increase simultaneously the temperature also increases. As the preceding graph makes evident, the propanol-filled air hole produces superior results than the air-filled air hole for the suggested PCF. After filling propanol, the temperature reaches its maximum value 84.2 ^{o}C at a wavelength 1.8 (μm) and that of for air filling PCF the temperature reaches its maximum value of 70.8 ^{o}C at the same wavelength. Figs. 4 and 5 illustrates how the birefringence and temperature both changes upward and is linearly proportional to wavelength which varies from 1.0 μm to 1.8 μm. It is possible to fit the relationship between the birefringence (B) and the temperature (T) as follows: $B = 7{,}51 \times 10^{-6}T + 12{,}9 \times 10^{-4}$ [17]. Additionally, it is evident from these simulation results that the propanol filled air holes PCF under study is capable of higher birefringence and temperature when compared to air filled PCF.

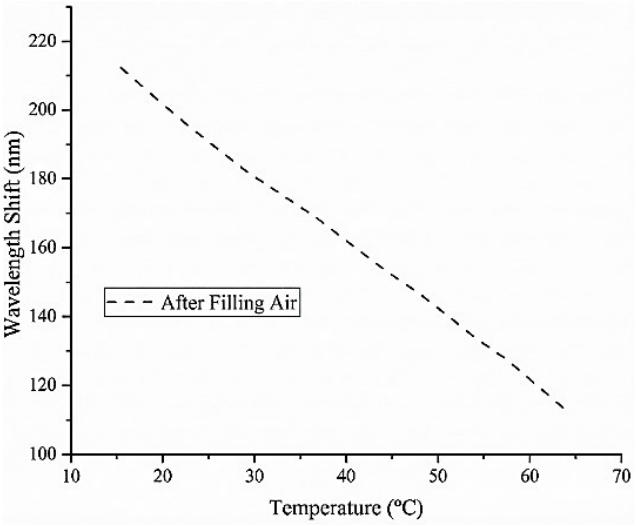

Fig. 6. Wavelength Shift (nm) vs Temperature (^{o}C) graph for air filled core

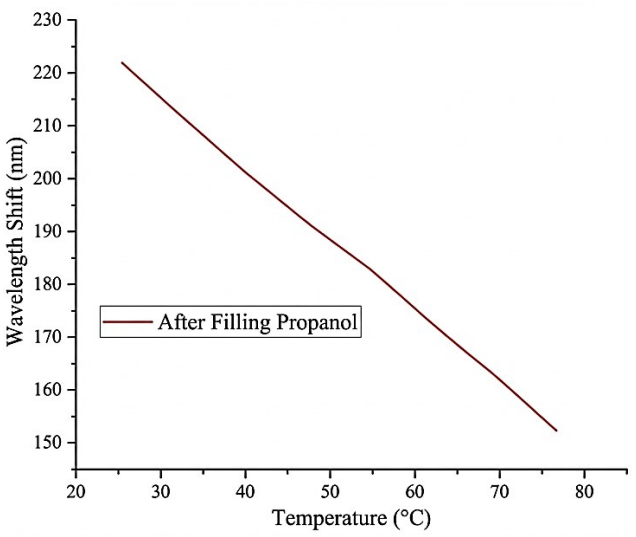

Fig. 7. Wavelength Shift (nm) vs Temperature (^{o}C) graph for propanol filled core (colour online)

Figs. 6 and 7 depict the graph of wavelength shift versus temperature of the designed PCF for both air filled and propanol filled core. The value of wavelength shift decreases from 212.2 nm to 113.3 nm with the increase in temperature from 15.4 °C to 63.7 °C for air filled core. Similarly for propanol filled core, the value of wavelength shift decreases from 221.8 nm to 152.3 nm with the increase in temperature from 25.4 °C to 76.6 °C. Consequently, for a given wavelength, we can calculate the dip wavelength shift brought on by the temperature variation as $\Delta\lambda_{dip}=\lambda\frac{\Delta B}{B}\sigma$ [23] where value of σ is assume to be 1 and $\frac{\Delta B}{B}$ signifies relative birefringence.

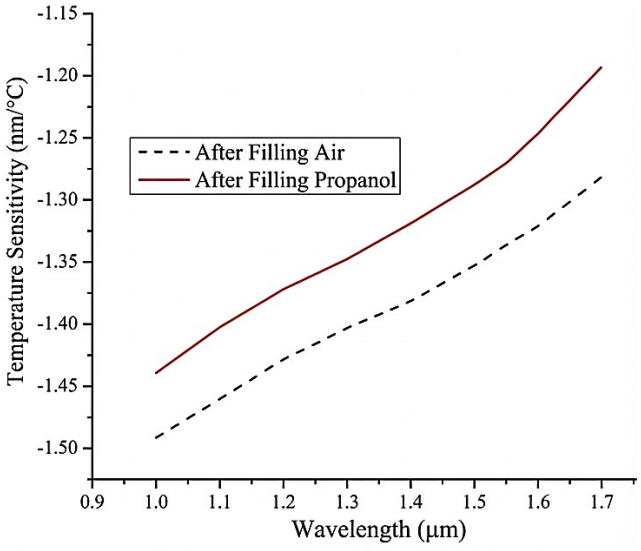

Fig. 8. Temperature Sensitivity (nm/°C) vs Wavelength (μm) graph (colour online)

Temperature sensitivity is one of the major parameters for E-shaped PCF used for temperature sensor. The formula used to calculate the temperature sensitivity [13] is given below.

$$S(\lambda) = \frac{\triangle \lambda_{Peak}}{\Delta T} \quad (3)$$

where $\triangle \lambda_{Peak}$ = Variable quantities of resonance peaks or peak wavelength and ΔT = Variation in temperature.

The temperature sensitivity depends upon the wavelength and also, we can say that the temperature sensitivity is regulated by the wavelength which can be clearly seen from the graph in Fig. 8. From the above plotted graph, it can be clearly seen that as the wavelength rises from 1 µm to 1.7 µm the value of temperature sensitivity also increases from -1.49 nm/°C to -1.28 nm/°C for air filled core and that of propanol filled core the value ranges from -1.43 nm/ °C to 1.19 nm/°C. Here temperature sensitivity is determined by the value of resonance wavelength shifts, higher value of temperature is reached when the resonance peak shifts more. The maximum calculated value of the sensitivity of temperature is -1.19 nm/°C for propanol and that of for air filled PCF is -1.28 nm/°C at wavelength 1.7 µm.

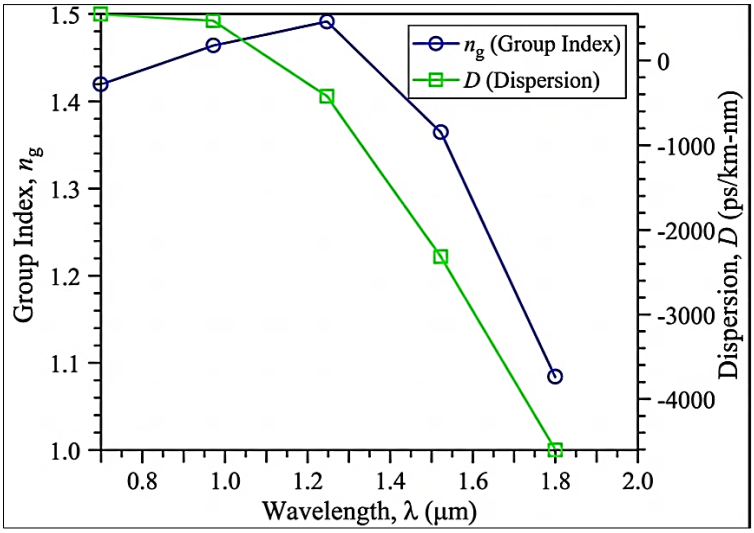

Fig. 9(a). Dispersion graph for propanol filled (colour online)

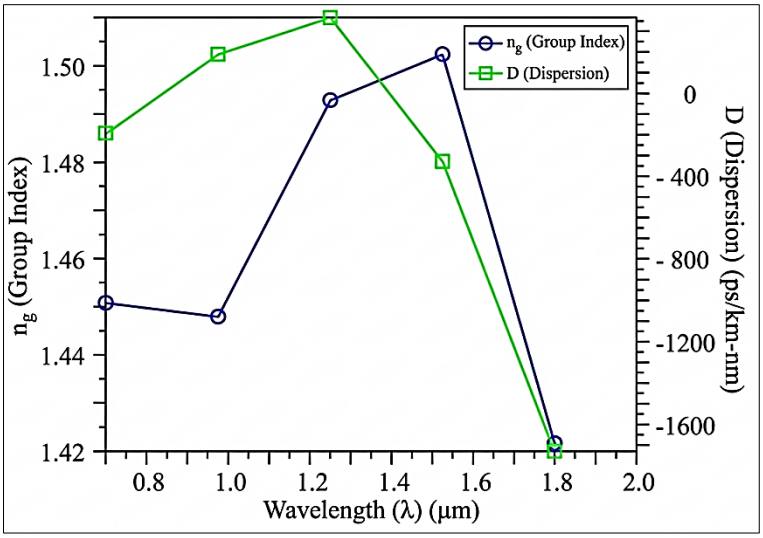

Fig. 9(b). Dispersion graph for air filled (colour online)

Dispersion is the one of the major concerning issues of the E-shaped PCF which can simply be regulated by changing the size of air hole and the material used in the cladding. The dispersion can be obtained from the formula [14-21] given below:

$$D = -\frac{\lambda}{c}\frac{d^2 \mathrm{Re}[n_{eff}]}{d\lambda^2} \quad (4)$$

where, Re [n_{eff}] denotes the real part of refractive index.

The graph depicted above in Figs. 9(a) and 9(b) is the highly negative dispersion graph. The value is highly negative for propanol filled air hole which is equal to -4000 ps/nm-km at a wavelength 1.8 μm. But the dispersion value for air filled in the air hole of the designed PCF is -1600 ps/nm-km at the same wavelength of 1.8 μm. It is clearly visualized in Fig. 9(a), that the graph slightly increases from wavelength 0.8 to 1.4 μm and then it sharply decreases at wavelength 1.8 μm for its highly negative value of dispersion. Similarly in Fig. 9(b) it is visualized that at a certain wavelength of 1.6 μm the graph sharply decreases and reaches its minimum value of (-1600) which is highly negative. In the above dispersion graph green colour line signifies dispersion (D) and blue colour signifies group index (n_g) which can be explained by considering the relationship $n_g = n_{eff} - \lambda.(dn_{eff}/d\lambda)$ [18] where n_{eff} is the waveguide's effective index. Birefringent PCFs offer advantages like high sensitivity and low temperature cross-sensitivity, but have limitations like complex fabrication and high cost, whereas FBGs are simple, cost-effective, and widely used, but suffer from temperature-strain cross-sensitivity [22].

Table 1. Analysis of the value of birefringence, temperature and temperature sensitivity for the proposed design with the existing PCF

Design PCF	**References**	**Birefringence**	**Dispersion (ps/nm-km)**	**Temperature range (˚C)**	**Temperature Sensitivity (nm/˚C)**
Alcohol Filled air hole	[16]	-	-	45-75	0.00165
Ethanol and Glycerin Filled airhole	[14]	-	-	20-50	0.00363
Toluene filled air hole	[6]	-	-	20-100	0.00651
PDMS Coated	[20]	-	-	35-65	-0.255
Propanol Filled air hole	[Proposed design]	7.62×10-2	-4000	25.4-76.6	-1.192
Air Filled air hole	[Proposed design]	6.61×10^{-2}	-1600	15.4-63.7	-1.352

Table 1 shows the comparative analysis of different parameter such as temperature, and its sensitivity, dispersion and birefringence of the proposed design with the exiting temperature sensor paper. It can be clearly seen from the above table that the propanol filled air hole reaches maximum temperature sensitivity of -1.192 nm/°C.

4. Conclusion

A highly birefringent E-Shaped PCF is designed to sense the temperature in which air is filled in the inner ring of PCF and compared its value with the propanol -filled PCF. Using (FEM) finite element method, all the required characteristics of the E-shaped PCF are numerically investigated and designed in the R-soft software. The main objective of the proposed design is to achieve improved sensitivity in wide range of temperature. The designed PCF focuses on their potential as next-generation sensors that can overcome the drawbacks of conventional temperature sensor while providing greater functionality and versatility. This type of PCF is widely used to monitor and control the structural health of the food, pharmaceutical, aerospace, and civil engineering industries. Different parameters such as birefringence, temperature and temperature sensitivity are calculated at a different wavelength ranging from 1 μm to 1.8 μm. The higher value of birefringence at 1.8 μm wavelength is 7.62×10-2, which is calculated after filling propanol, while it is 6.61×10-2 for air. The sensitivity of the designed structure ranges from -1.43 nm/°C to -1.19 nm/°C after filling propanol in the wavelength 1 μm to 1.7 μm range. And the sensitivity of the designed structure ranges from -1.49 nm/°C to -1.28 nm/°C for air filled PCF in the same wavelength from 1 μm to 1.7 μm range which is applicable for sensing the temperature.

References

[1] T. Yang, E. Wang, H. Jiang, Z. Hu, K. Xie, Opt. Express **23**(7), 8329 (2015).
[2] Sapna Tiwari, Gaurav Kumar Bharti, Ahmad S. Abdullah, Optoelectron. Adv. Mat. **19**(9-10), 421 (2025).
[3] Y.-H. Chang, Y.-Y. Jhu, C.-J. Wu, Optics Communications **285**(6), 1501 (2012).
[4] G. N. Nirala, J. B. Maurya, B. A. Kumar, J. K. Baral, Optoelectronic. Adv. Mat. **19**(3-4), 142 (2025).
[5] J. K. Yadav, S. K. Tripathy, Gaurav Kumar Bharti, Neeraj Kumar, Eur. Phys. J. Plus **139**(4), 308

(2024).
[6] U. Biswas, J. K. Rakshit, J. Das, Gaurav Kumar Bharti, Bhuvneshwer Suthar, Angela Amphawan, Monia Najjar, Silicon **13**, 885 (2021).
[7] S. Olyaee, A. A. Dehghani, Sens. Lett. **11**(10), 1854 (2013).
[8] C. Lee, J. Thillaigovindan, Appl. Optics **48**(10), 1797 (2009).
[9] B. Purohit, A. Kumar, K. Mahato, P. Chandra, Current Opinion in Biomedical Engineering **13**, 42 (2020).
[10] M. Zaynetdinov, E. M. See, B. Geist, G. Ciovati, H. D. Robinson, V. Kochergin, IEEE Sens. J. **15**(3), 1908 (2015).
[11] C. Du, Q. Wang, Y. Zhao, J. Li, Opt. Fiber Technol. **34**, 12 (2017).
[12] Y. Cui, P. Shum, D. J. J. Hu, G, Wang, G. Humbert, X. Q. Dinh, IEEE Photonics J. **4**(5), 1801 (2012).
[13] X. Yang, Y. Lu, B. Liu, J. Yao, IEEE Photonics J. **10**(2), 1 (2018).
[14] S. Weng, L. Pei, J. Wang, T. Ning, J. Li, Photonic Research **5**(2), 103 (2017).
[15] Y. Gao, C. Sima, J. Cheng, B. Cai, K. Yuan, Z. Lian, M. Smietana, P. Lu, D. Liu, Optics Communications **450**, 172 (2019).
[16] S. Qiu, J. Yuan, X. Zhou, Y. Qu, B. Yan, Q. Wu, K. Wang, X. Sang, K. Long, C. Yu, Optics Communications **477**, 126357 (2020).
[17] S. Das, M. De, V. K. Singh, Optical Fiber Technology **53**, 1 (2019).
[18] B. K. Paul, K. Ahmed, M. T. Rani, K. P. S. Pradeep, F. A. Al-Zahrani, Alexandria Engineering Journal **61**, 2799 (2022).
[19] G. Wang, Y. Lu, X. Yang, L. Duan, J. Yao, Appl. Optics **58**(8), 2132 (2019).
[20] R. Boufenar, M. Bouamar, A. Hocini, Photonics and Nanostructures – Fundamentals and Applications **24**, 47 (2017).
[21] E. Dulkeith, F. Xia, L. Schares, W. M. J. Green, Y. A. Vlasov, Opt. Express **14**(9), 3853 (2006).
[22] V. R. Balaji, M. A. Ibrar Jahan, Gaurav Kumar Bharti, Archana Yadav, Srujana, Rajini V. Honnungar, FBG Sensor Applications in Aerospace Engineering, in Carlos Marques, Raja V. L. N. Sridhar, Santosh Kumar (Eds.), "Advanced Optical Sensors for Aerospace Applications", Springer, p. 97, 2025.

*Corresponding author: manisha17n@gmail.com